SPC summary: QCD Thermodynamics (Hot Nuclear Physics track)

Alexei Bazavov
Michigan State University

USQCD All Hands Meeting
MIT Apr 21 - 22 2022

QCD phase diagram

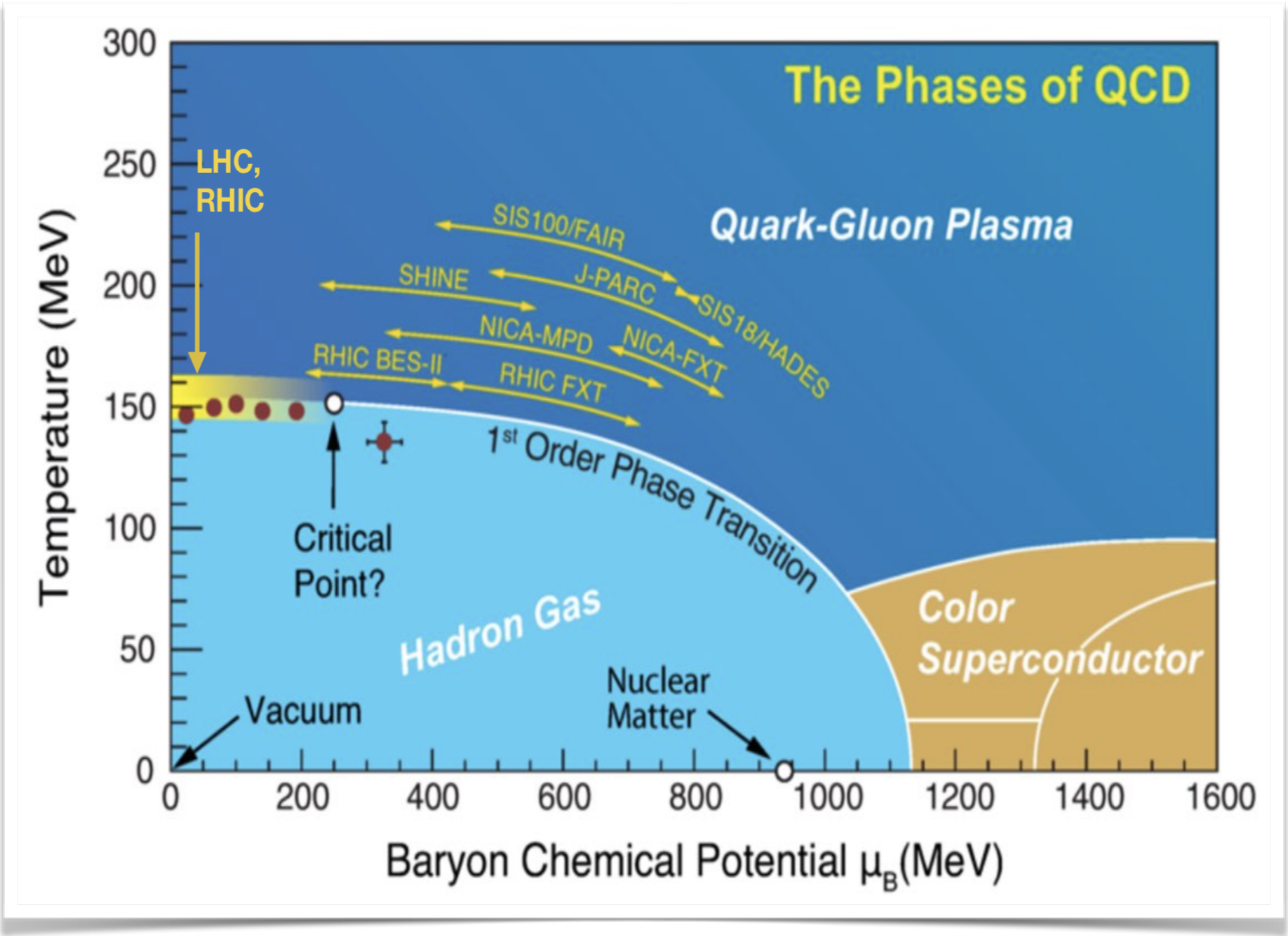

USQCD whitepaper

Hot-dense Lattice QCD: USQCD whitepaper 2018

In light of the ongoing and future heavy-ion experimental programs at RHIC and LHC, this USQCD whitepaper outlines the opportunities for, prospects of and challenges to the hot-dense lattice QCD calculations in addressing the issues: (i) phases and properties of baryon-rich QCD, (ii) microscopy of QGP using heavy-quark probes, (iii) nature of QCD phase transitions, (iv) electromagnetic probes of QGP, (v) jet energy loss in and viscosities of QGP.

- RHIC: Beam Energy Scan II, sPHENIX
- Two USQCD proposals this year (one new, one continuing)

Cumulants of conserved charge fluctuations

- Taylor expansion of the pressure:

$$\frac{P}{T^4} = \frac{1}{VT^3} \ln \mathcal{Z}(T, V, \vec{\mu}) = \sum_{i,j,k=0}^{\infty} \frac{\chi_{ijk}^{BQS}}{i!j!\,k!} \hat{\mu}_B^i \hat{\mu}_Q^j \hat{\mu}_S^k$$

- Generalized susceptibilities:

$$\chi_{ijk}^{BQS} = \frac{1}{VT^3} \frac{\partial \ln \mathcal{Z}(T, V, \vec{\mu})}{\partial \hat{\mu}_B^i \partial \hat{\mu}_Q^j \partial \hat{\mu}_S^k} \Bigg|_{\vec{\mu}=0}, \quad i+j+k \text{ even}$$

- Additional constraints enforce strangeness neutrality $n_S = 0$ and fixed ratio of electric charge to the baryon number $n_Q/n_B = r$

$$\hat{\mu}_Q(T, \mu_B) = q_1(T)\hat{\mu}_B + q_3(T)\hat{\mu}_B^3 + q_5(T)\hat{\mu}_B^5 + \ldots$$
$$\hat{\mu}_S(T, \mu_B) = s_1(T)\hat{\mu}_B + s_3(T)\hat{\mu}_B^3 + s_5(T)\hat{\mu}_B^5 + ..$$

- Taylor series in only baryon chemical potential

Second-order cumulants revisited at $\mu = 0$

- Significant update of statistics
- Several cutoffs: $N_\tau = 6,8,12,16$
- Fully controlled continuum limit
- Comparison with statistical models, updated QMHRG2020
- Model sensitivity to the spectrum, in particular, in the strange baryon sector

Bollweg et al. (HotQCD), PRD 104 (2021)

Second-order cumulants revisited at $\mu = 0$

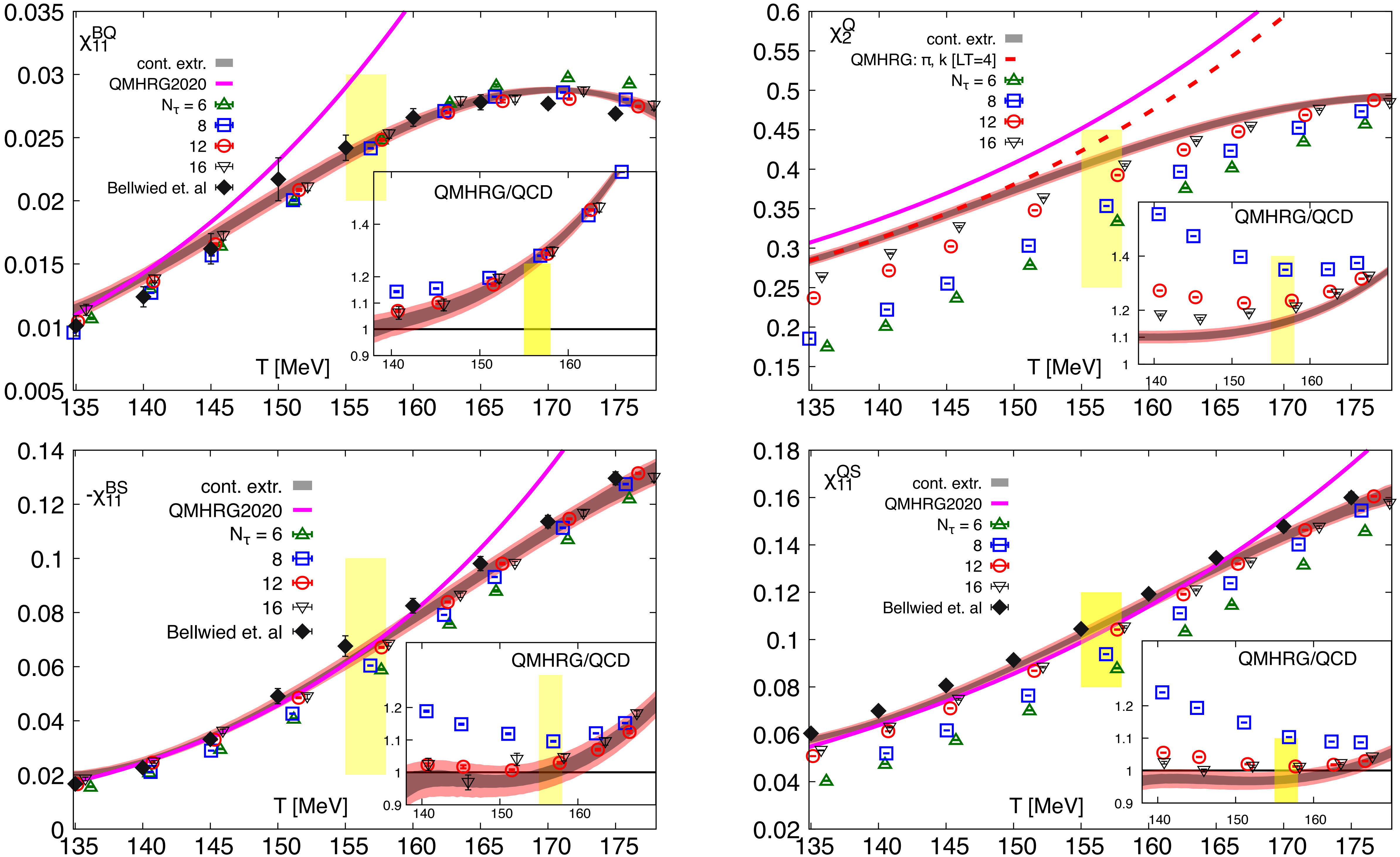

Bollweg et al. (HotQCD), PRD 104 (2021)

Second-order cumulants revisited at $\mu = 0$

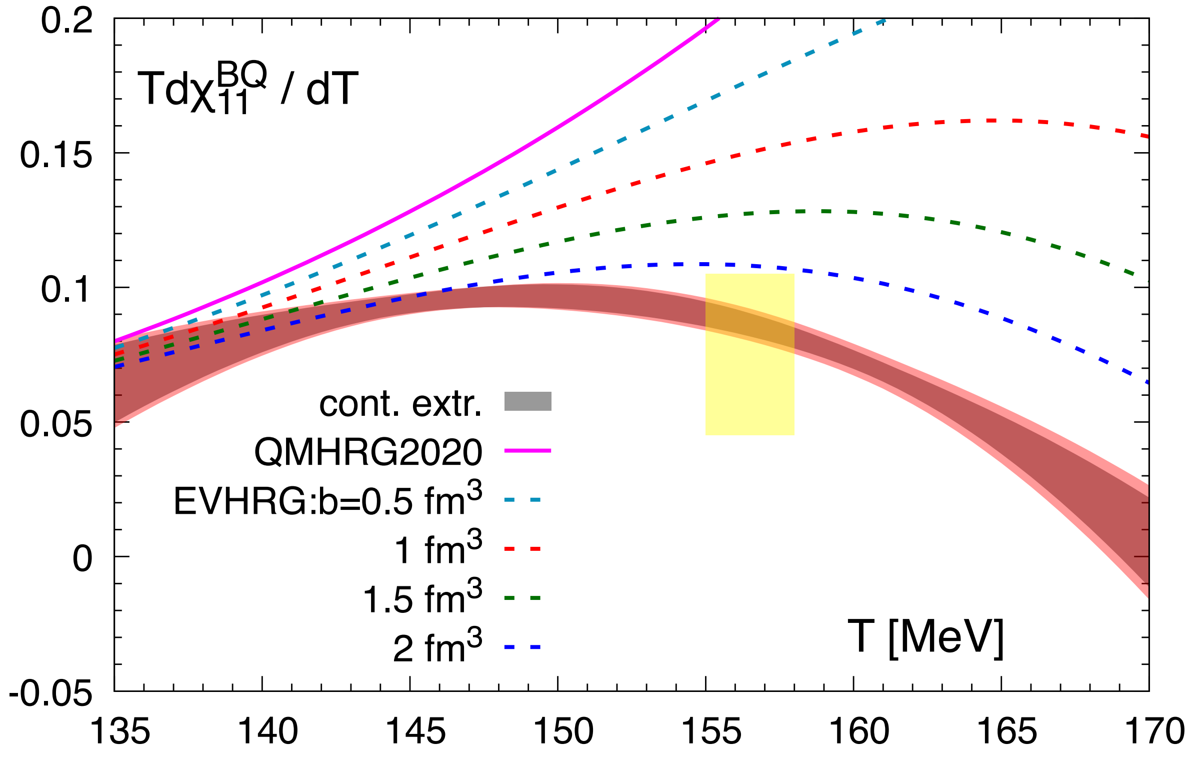

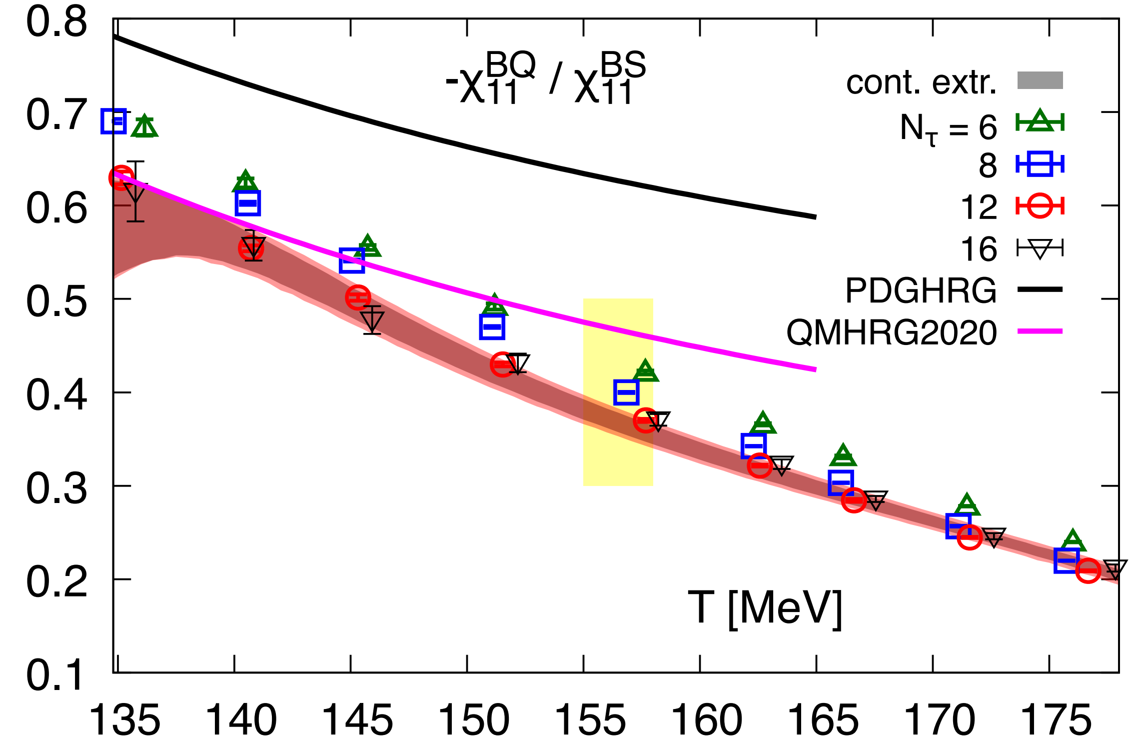

- Temperature derivative of the baryon number - electric charge correlations in lattice QCD compared with the HRG with excluded volume corrections (left)
- Ratio of baryon number - electric charge to baryon number - strangeness correlation in lattice QCD and HRG with different spectrum (right)

Bollweg et al. (HotQCD), PRD 104 (2021)

Second-order cumulants revisited at $\mu = 0$

- QMHRG2020 provides a good description of strangeness fluctuations and correlations with baryon-number and electric charge fluctuations, deviations are less than 10% for $135 \text{ MeV} < T < T_{pc} = 156.5 \text{ MeV}$
- The largest differences between QCD results and HRG model calculations, about 20% at T_{pc}, are for correlations between net baryon-number and electric charge
- Stringent constraints on phenomenological models

Bollweg et al. (HotQCD), PRD 104 (2021)

Second-order cumulants revisited at $\mu \neq 0$

- Improved statistics on χ_{ijk}^{BQS} with $i + j + k \leq 8$
- Several cutoffs: $N_\tau = 6{,}8{,}12{,}16$
- Fully controlled continuum limit
- Padé approximations for the Taylor series, poles and convergence analysis
- Pressure (0th order) and first and second order cumulants at $\mu_B \neq 0$

$$n_B = \frac{\partial P/T^4}{\partial \hat{\mu}_B}$$
$$\chi_2^B = \frac{\partial^2 P/T^4}{\partial \hat{\mu}_B^2}$$

Bollweg et al. (HotQCD), 2202.09184

Second-order cumulants revisited at $\mu \neq 0$

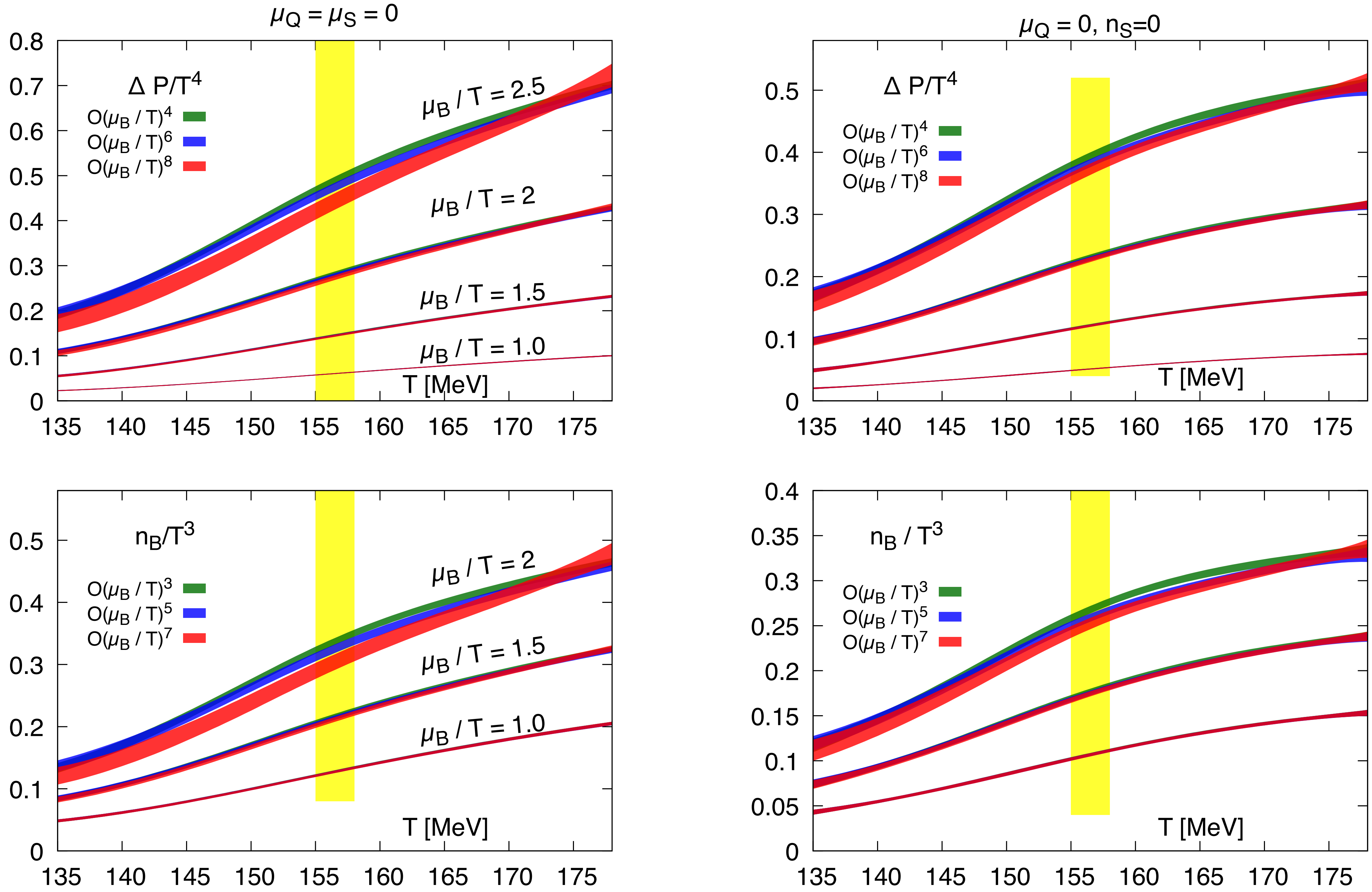

- Contribution to the pressure at $\mu_B \neq 0$ (top) and net baryon-number density (bottom)

Bollweg et al. (HotQCD), 2202.09184

Second-order cumulants revisited at $\mu \neq 0$

- Padé approximations

$$\frac{(\Delta P(T,\mu_B)/T^4)P_4}{P_2^2} = \sum_{k=1}^{\infty} c_{2k,2}\bar{x}^{2k} \ ,$$
$$= \bar{x}^2 + \bar{x}^4 + c_{6,2}\bar{x}^6 + c_{8,2}\bar{x}^8 + ..$$

$$c_{6,2} = \frac{P_6 P_2}{P_4^2} = \frac{2}{5}\frac{\bar{\chi}_6^B \bar{\chi}_2^B}{(\bar{\chi}_4^B)^2} \ ,$$
$$c_{8,2} = \frac{P_8 P_2^2}{P_4^3} = \frac{3}{35}\frac{\bar{\chi}_8^B (\bar{\chi}_2^B)^2}{(\bar{\chi}_4^B)^3}$$

$$\bar{x} = \sqrt{\frac{P_4}{P_2}}\ \hat{\mu}_B \equiv \sqrt{\frac{\bar{\chi}_0^{B,4}}{12\bar{\chi}_0^{B,2}}}\ \hat{\mu}_B$$

$$P[2,2] = \frac{\bar{x}^2}{1-\bar{x}^2} \ ,$$
$$P[4,4] = \frac{(1-c_{6,2})\bar{x}^2 + (1-2c_{6,2}+c_{8,2})\,\bar{x}^4}{(1-c_{6,2}) + (c_{8,2}-c_{6,2})\bar{x}^2 + (c_{6,2}^2 - c_{8,2})\bar{x}^4}$$

Bollweg et al. (HotQCD), 2202.09184

Second-order cumulants revisited at $\mu \neq 0$

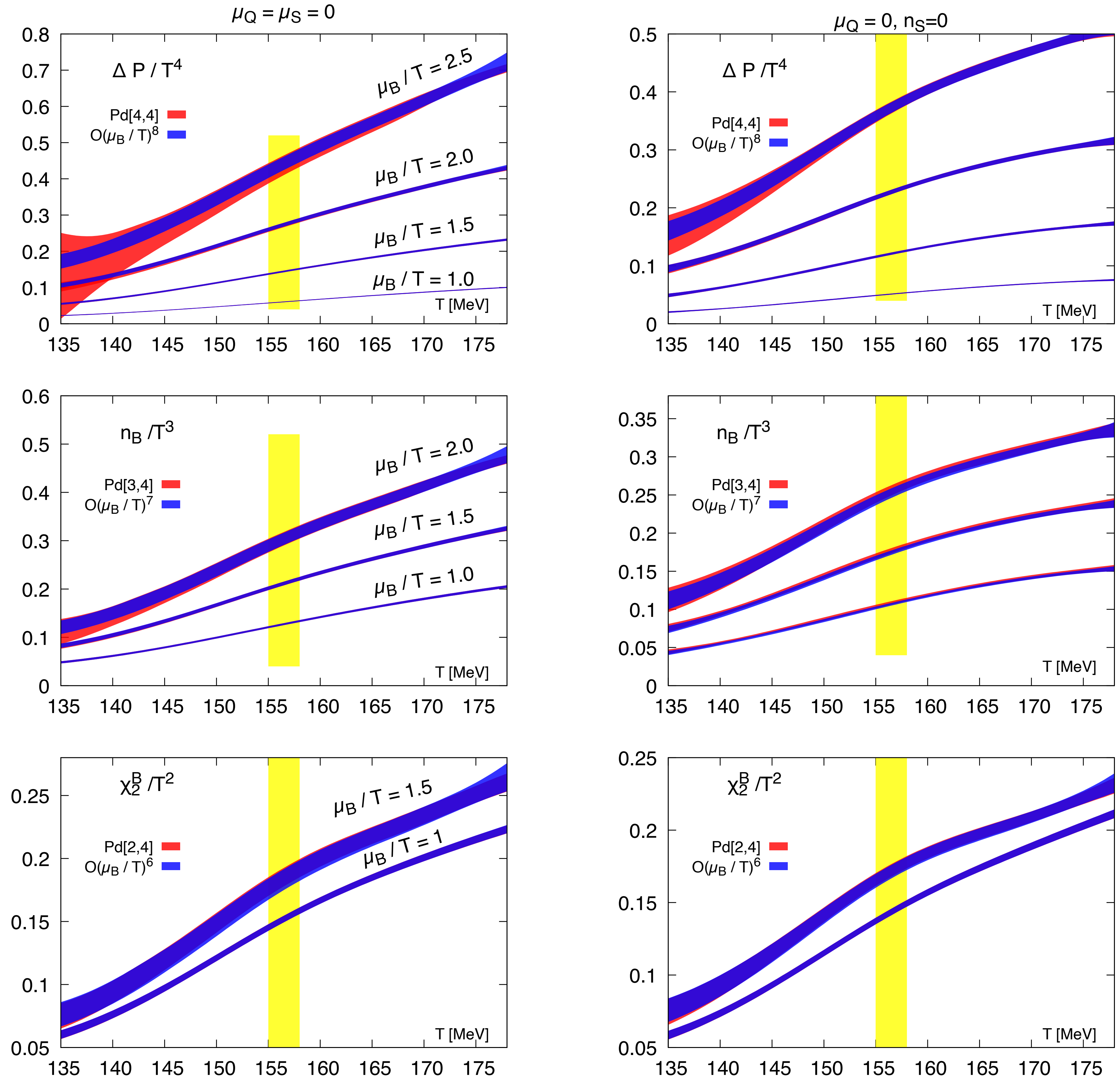

Second-order cumulants revisited at $\mu \neq 0$

- [4,4] Padé approximant — reproduces eighth-order Taylor series for the pressure
- Only complex poles in the interval 135 MeV $\leq T \leq$ 165 MeV
- A possible critical point may only be at $T \leq$ 135 MeV
- Agreement between Padé and Taylor series for pressure — $\mu_B \leq 2.5T$, baryon number density — $\mu_B \leq 2T$, second order cumulant χ_2^B — $\mu_B \leq 1.5T$

Resummation of Taylor series

- Pressure, again

$$\frac{\Delta P_N^E}{T^4} = \sum_{n=1}^{N} \frac{\chi_n^B}{n!}\left(\frac{\mu_B}{T}\right)^n \qquad \chi_n^B(T) = \frac{1}{VT^3}\,\frac{\partial^n \ln Z(T,\mu_B)}{\partial(\mu_B/T)^n}\bigg|_{\mu_B=0}$$

- Individual contributions to the cumulants

$$\left\langle D_i^a D_j^b \cdots D_k^c \right\rangle \text{ with } i\cdot a + j\cdot b + \cdots + k\cdot c = n$$

$$D_n(T) = \bar{D}_n \cdot n! = \frac{\partial^n \ln\det[M(T,\mu_B)]}{\partial(\mu_B/T)^n}\bigg|_{\mu_B=0}$$

- In continuum: integrated n-point function of the conserved current

$$D_n = \int \mathrm{d}\mathbf{x_1}\cdots\mathrm{d}\mathbf{x_n} J_0(\mathbf{x_1})\cdots J_0(\mathbf{x_n})$$

Mondal, Mukherjee, Hegde, PRL 128 (2022)

Resummation of Taylor series

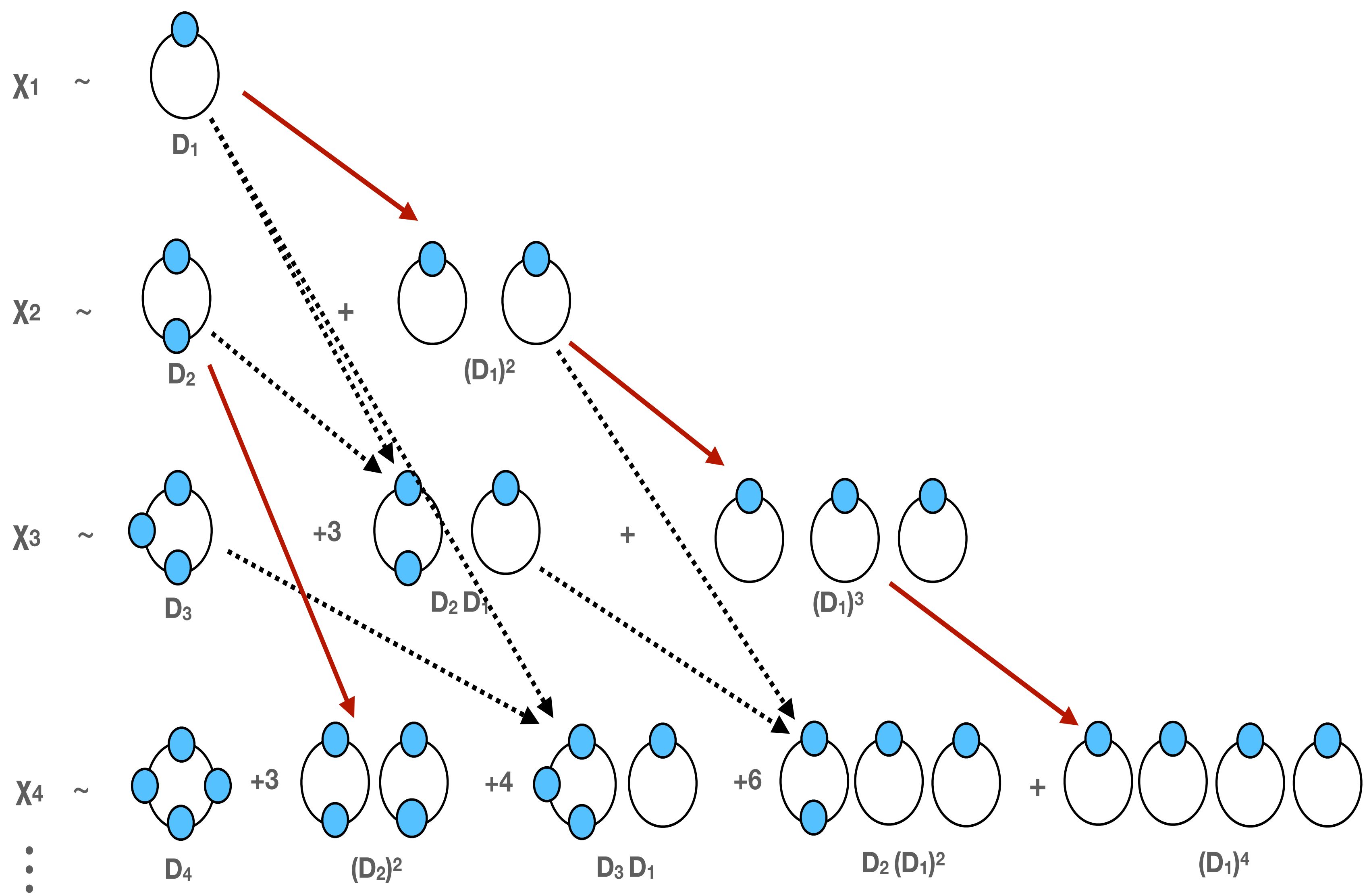

$$\frac{\Delta P_N^R}{T^4} = \frac{1}{T^3 V} \ln \left\langle \exp\left[\sum_{n=1}^{N} \bar{D}_n \left(\frac{\mu_B}{T} \right)^n \right] \right\rangle$$

Mondal, Mukherjee, Hegde, PRL 128 (2022)

Resummation of Taylor series

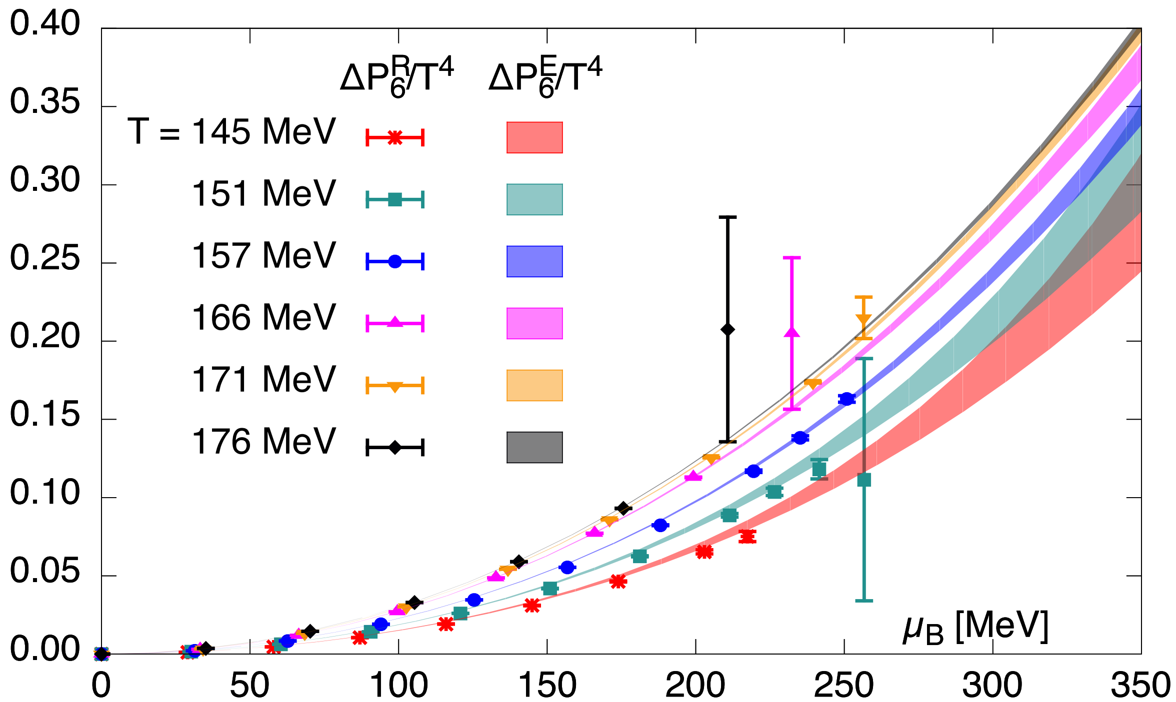

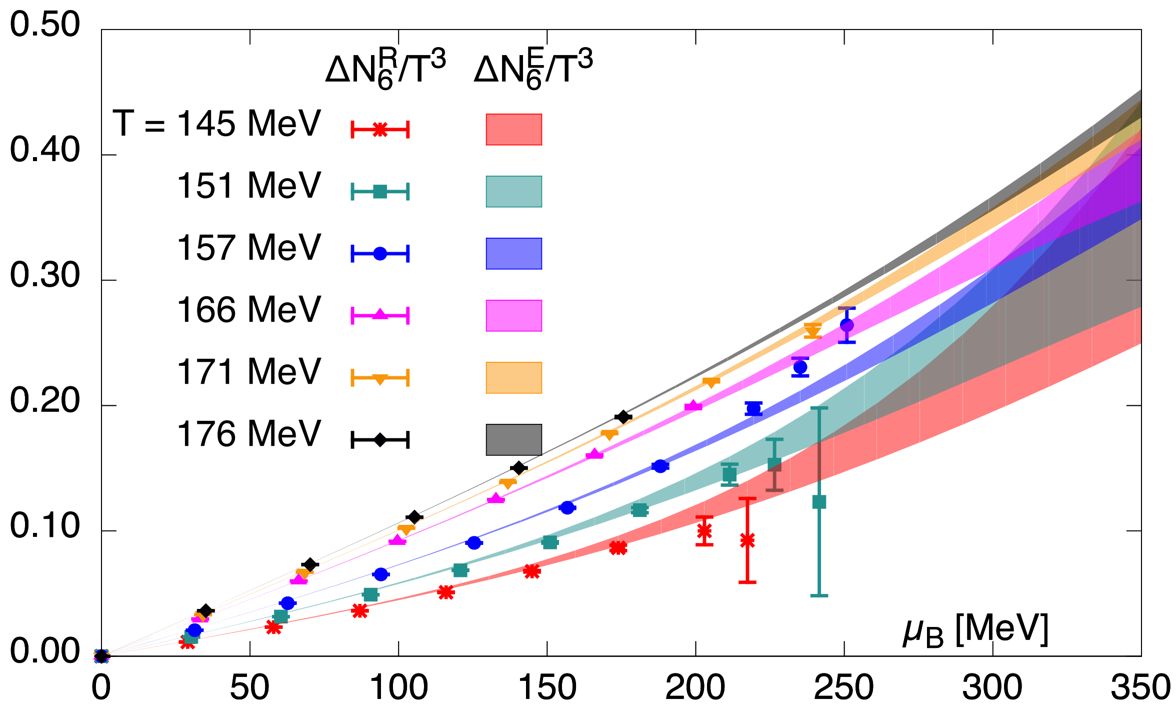

- Comparison of the Taylor expansion and resummed series for the pressure (top) and the baryon number density (bottom)
- Can be generalized to multi-parameter expansion, i.e. T, μ_B
- Estimates of the average phase of Z — severity of the sign problem

Mondal, Mukherjee, Hegde, PRL 128 (2022)

$U_A(1)$ anomaly and eigenvalue spectrum

$$\begin{tikzcd}
\pi : \bar{q}\gamma_5 \frac{\tau}{2} q \arrow[rr, leftrightarrow, "SU_L(2) \times SU_R(2)"] \arrow[d, leftrightarrow, "U_A(1)"'] & & \sigma : \bar{q}q \arrow[d, leftrightarrow, "U_A(1)"] \\
\delta : \bar{q}\frac{\tau}{2} q \arrow[rr, leftrightarrow, "SU_L(2) \times SU_R(2)"'] & & \eta : \bar{q}\gamma_5 q
\end{tikzcd}$$

- χ_π and χ_σ become degenerate when chiral symmetry is restored
- $\chi_\pi - \chi_\delta$ indicates the breaking/restoration of the $U_A(1)$ symmetry

$$\chi_\pi - \chi_\delta = \chi_{dis} + \left(\chi_\pi - \chi_\sigma\right)$$

$$\chi_\pi - \chi_\delta \quad = \quad \int_0^\infty \mathrm{d}\lambda \frac{4m^2 \ \rho(\lambda, m)}{(\lambda^2 + m^2)^2} \qquad \chi_{\mathrm{disc}} = \int_0^\infty \mathrm{d}\lambda \ \frac{4m_l \ \ \partial\rho/\partial m_l}{\lambda^2 + m_l^2}$$

Chiral limit and axial anomaly at high temperature

- Currently ongoing calculations, PI: Petreczky, type A, “The chiral limit of (2+1)-flavor QCD and the axial anomaly at high temperature”
- Study of the Dirac eigenvalue spectrum based on the new relations proposed in Ding et al., PRL 126 (2021)

$$\frac{V}{T}\frac{\partial\rho}{\partial m_l} = \int_0^\infty \mathrm{d}\lambda_2\, \frac{4m_l\, C_2(\lambda,\lambda_2;m_l)}{\lambda_2^2+m_l^2}\,,$$

$$\frac{V}{T}\frac{\partial^2\rho}{\partial m_l^2} = \int_0^\infty \mathrm{d}\lambda_2\, \frac{4(\lambda_2^2-m_l^2)\, C_2(\lambda,\lambda_2;m_l)}{(\lambda_2^2+m_l^2)^2} + \int_0^\infty \mathrm{d}\lambda_2\,\mathrm{d}\lambda_3\, \frac{(4m_l)^2\, C_3(\lambda,\lambda_2,\lambda_3;m_l)}{(\lambda_2^2+m_l^2)(\lambda_3^2+m_l^2)}$$

$$C_n(\lambda_1,\cdots,\lambda_n;m_l) = \left\langle \prod_{i=1}^{n}\left[\rho_U(\lambda_i)-\langle\rho_U(\lambda_i)\rangle\right]\right\rangle$$

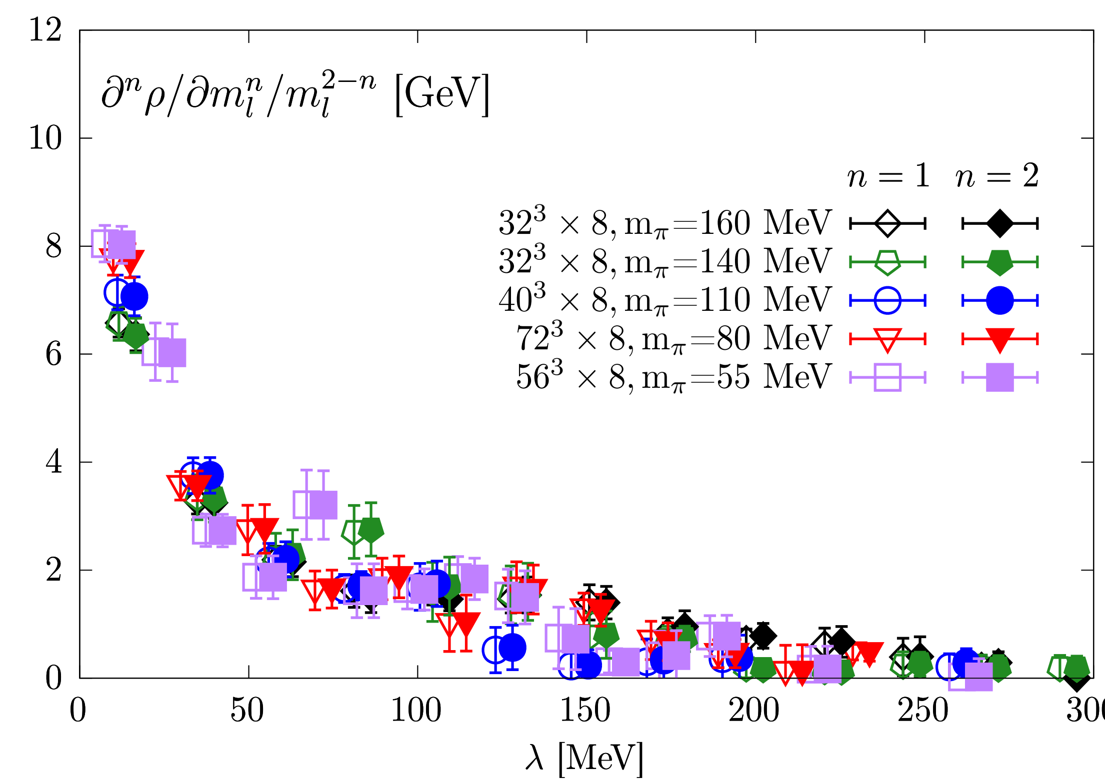

Chiral limit and axial anomaly at high temperature

- Currently ongoing calculations, PI: Petreczky, type A, “The chiral limit of (2+1)-flavor QCD and the axial anomaly at high temperature”
- Study of the Dirac eigenvalue spectrum based on the new relations proposed in Ding et al., PRL 126 (2021)

- Preliminary results:
  Ding et al., Lattice 2021
  Ding et al., Lattice 2021

Bottomonium screening masses

- Meson spatial correlation functions

$$G(z,T) = \int_0^\infty \frac{2d\omega}{\omega} \int_{-\infty}^{\infty} dp_z e^{ip_z z} \sigma(\omega, p_z, T)$$

- Expect the screening mass at high T $\sim 2\sqrt{(\pi T)^2 + m_q^2}$
- Relativistic (HISQ) b quark

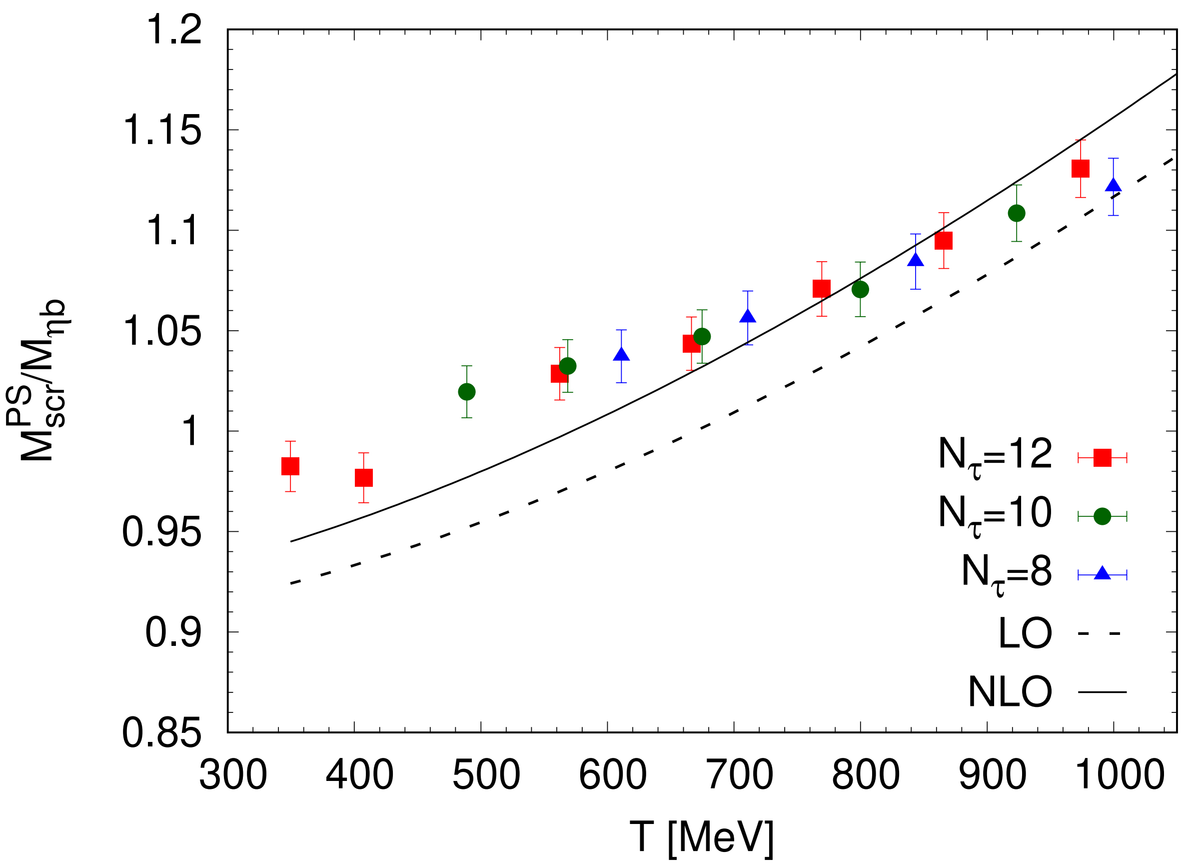

- Thermal modifications of η_b at $\sim T > 500$ MeV

Petreczky, Sharma, Weber, PRD 104 (2021)

Static quark potential at finite T

- Spectral decomposition of the Wilson loop

$$W_\Box(r,\tau,T) = \int d\omega e^{-\omega\tau} \rho_r(\omega,T)$$

- Cumulants of the correlation function

$$m_1(r,\tau,T) = -\partial_\tau \ln W(r,\tau,T),$$
$$m_n = \partial_\tau m_{n-1}(r,\tau,T), n > 1.$$

- Comparison with HTL-resummed perturbation theory

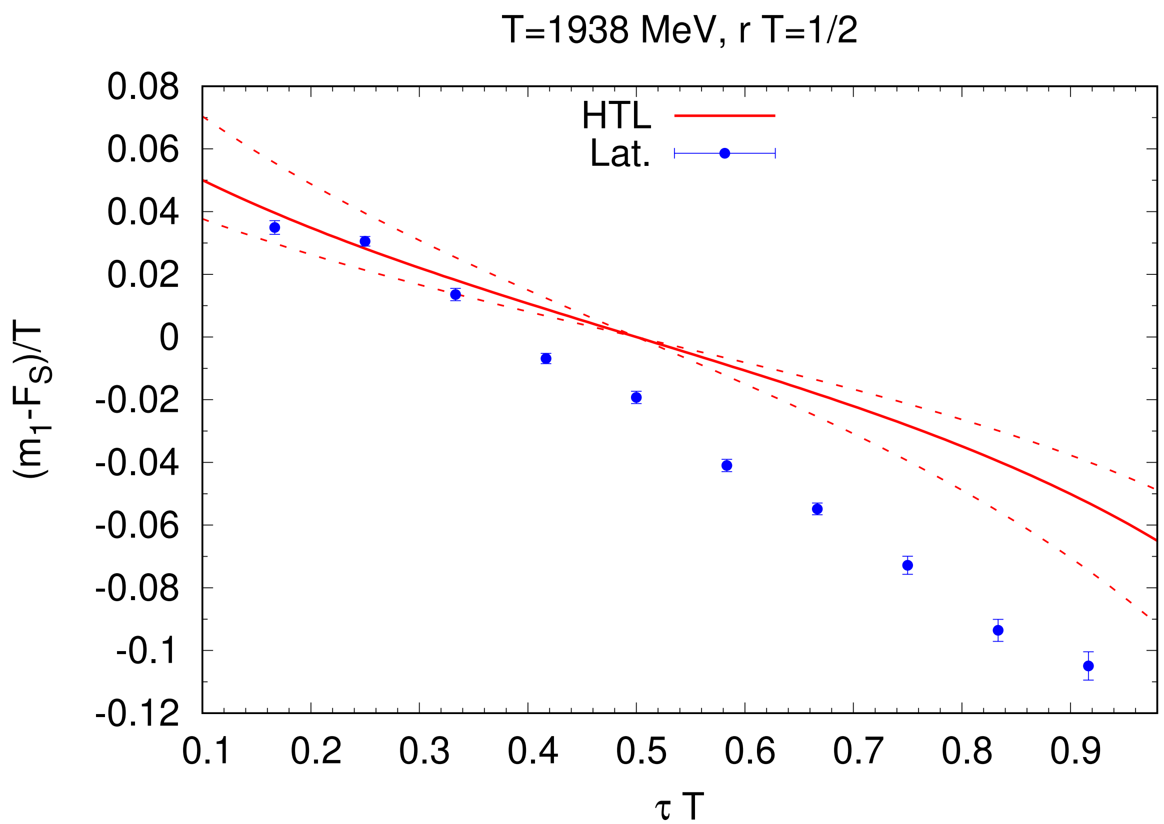

Bala et al. (HotQCD) PRD 105 (2022)

Static quark potential at finite T

- Extraction of the position Ω and width Γ of the dominant spectral peak structure encoded in the Wilson line correlators with four different methods: spectral function model fits with a Gaussian, HTL-inspired fit, the Pade approximation and Bayesian BR method.

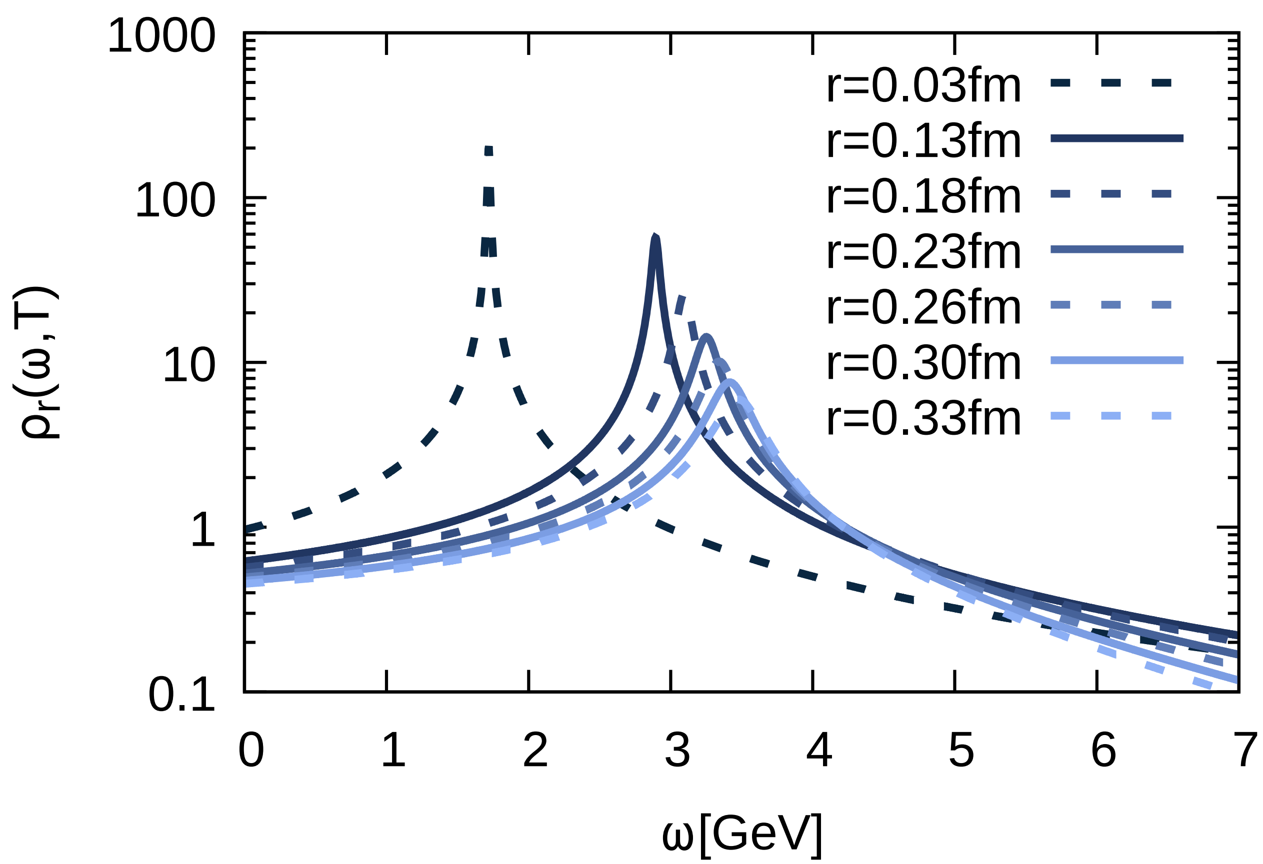

- Representative spectral function from Pade at $T = 407$ MeV

Bala et al. (HotQCD) PRD 105 (2022)

Static quark potential at finite T

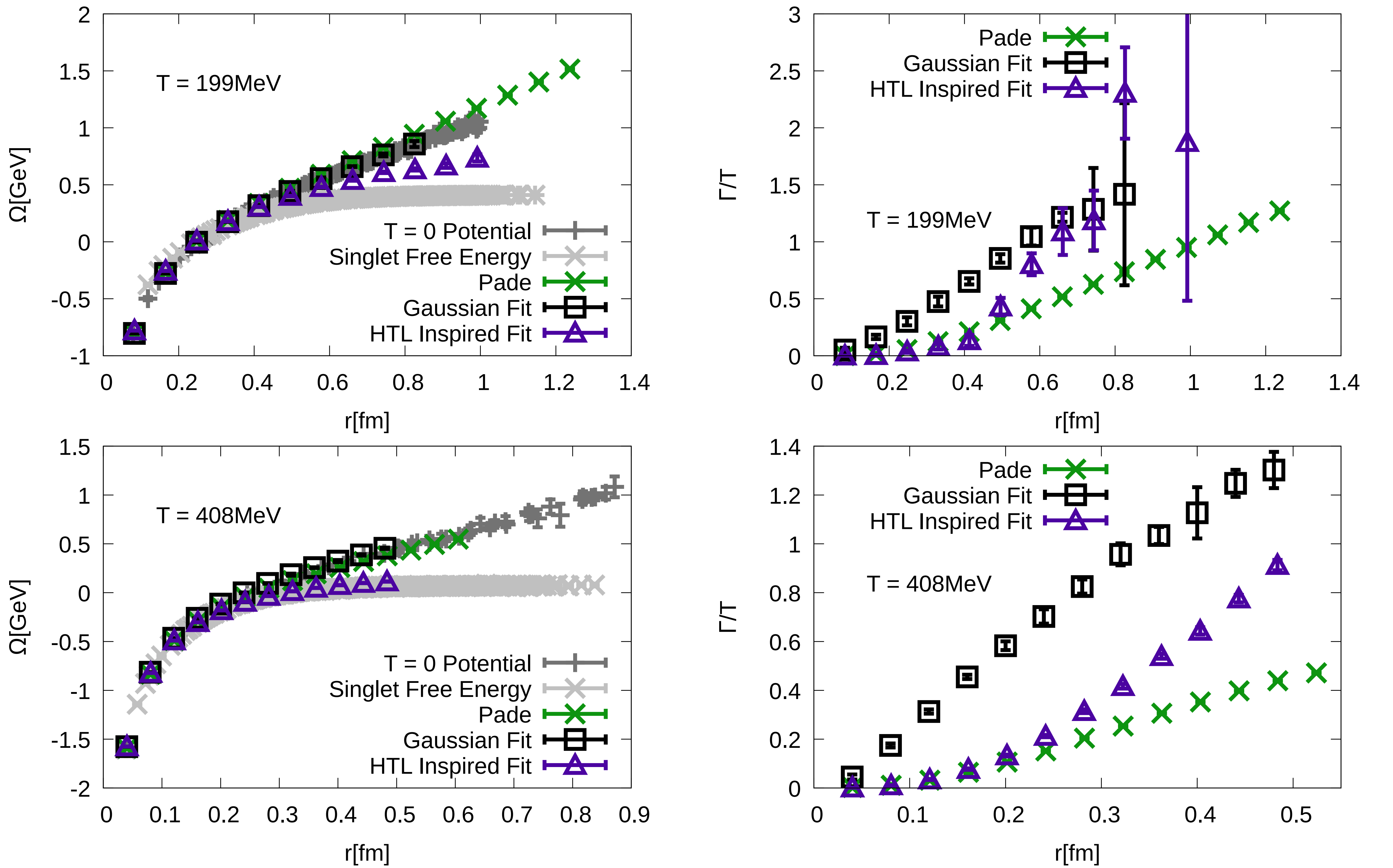

- Position (left) and width (right) of the spectral peak at $T = 119,\ 408$ MeV with different methods

Bala et al. (HotQCD) PRD 105 (2022)

Quarkonia spectral functions

- The in-medium properties and dissolution patterns are encoded in the spectral functions

$$\rho(\omega,\vec{p}) = \frac{1}{2\pi}(D^{>}(\omega,\vec{p}) - D^{<}(\omega,\vec{p})) = \frac{1}{\pi}\mathrm{Im}D^{R}(\omega,\vec{p})$$

- On the lattice we measure Euclidean correlation functions

$$G(\tau,\vec{p}) = \int d^3x e^{i\vec{p}.\vec{x}}\langle J(\tau,\vec{x})J(0,\vec{0})\rangle$$

- Need to solve an inverse problem to reconstruct the spectral function

$$G(\tau,\vec{p}) = \int_0^\infty d\omega\rho(\omega,\vec{p})K(\omega,\tau), \quad K(\omega,\tau) = \frac{\cosh(\omega(\tau - 1/2T))}{\sinh(\omega/2T)}$$

PI: Bazavov

- "Novel anisotropic pure gauge simulations and the spectrum of anisotropic staggered quarks"
- Continuation
- Pure gauge, anisotropic Highly Improved Staggered Quarks
- Focus: pure gauge generation, anisotropy tuning, studying aHISQ spectrum
- **Request:** 2.8 M Sky-core-hours

Anisotropy tuning, pion taste splittings

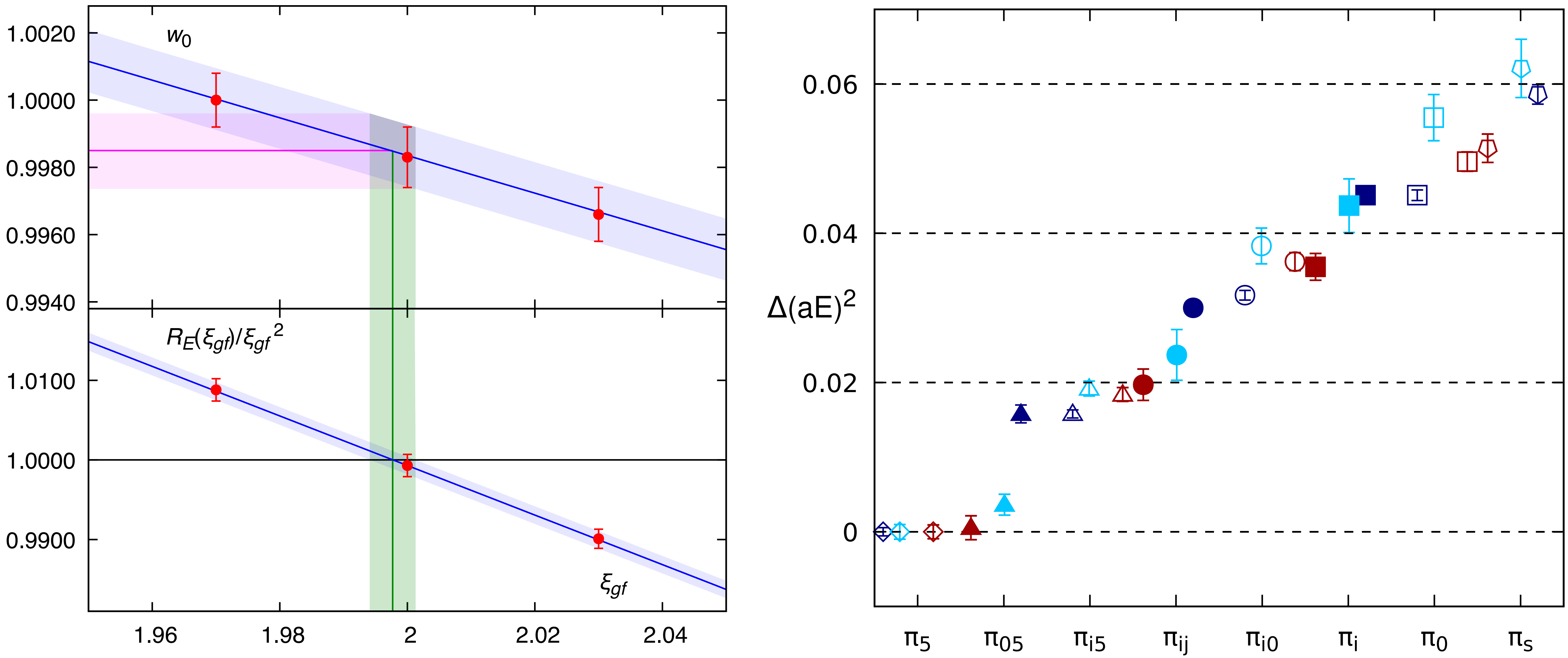

- Gauge anisotropy tuning with the gradient flow, WB, 1205.0781 (left)
- Splitting of the pion tastes from the Goldstone pion at renormalized fermion anisotropy $\xi_f = 1{,}2{,}4$ (right)

PI: Petreczky

- “The heavy quark diffusion coefficient in (2+1)-flavor QCD from lattice”
- New proposal
- Highly Improved Staggered Quarks
- Focus: gauge generation, several temperatures for $m_l/m_s = 1/5$ and physical, $64^3 \times N_\tau$ ensembles
- **Request:** 28.8 M KNL-core-hours + 0.87 M K80-GPU-hours